Chapter 3 Finite Element Model

3.1 Introduction

This chapter describes the FE model implemented in JAM and briefly documents the constitutive models available in the code. The work of Biot and other investigators is described, followed by a discussion of the equations implemented by Lewis and Schrefler and modifications that must be made to those equations. In addition, the equations are derived for the residuals. The five constitutive models available in JAM for modeling skeletal behavior are described. The algorithms required to numerically simulate the behavior of the three primary constituents of geomaterials, air, water and solids, are also documented in this chapter.

3.2 Effective Stress Mechanics

In Section 1.1, requirements for an advanced analysis tool were presented. An inherent assumption in the design of the analysis tool was that effective stress mechanics and a modified Biot theory were required. The following text defines effective stress mechanics terms and justifies the use of both effective stress mechanics and a modified Biot theory.

All porous geomaterials are composed of solids and pore fluids. Effective stress mechanics (Frederickson, et al. 1989) involves the "explicit consideration of the portions of the material stress carried by the porous soil or rock skeleton and by the fluid/gas phase constituents." Effective stress is the portion of the material stress that is transmitted through the solid phase of

the porous skeleton. The pore fluid pressure or pore pressure is the portion of the material stress transmitted through the pore fluids. In this document, we assume the only pore fluid constituents are air and water, and that they do not transmit shear stresses. In the absence of pore fluid pressure, e.g., a drained mechanical property test, effective stresses and total stresses are the same.

There are several compelling arguments for adopting effective stress mechanics in the analysis tool. The primary advantage is that the behavior of each constituent in a porous material, i.e., the solids, water, and air, is explicitly treated. Vigorous equations of state are available for water, air, and many solids. Since the equations of state of the constituents are well developed, the predominant uncertainty in modeling a porous material is limited to the skeletal constitutive model. This method allows the modeler to concentrate time and effort in improving just one area of material response, i.e., the skeletal constitutive model. There are other advantages also. An effective stress mechanics approach reduces the modeling effort for materials from inaccessible sites; only the drained skeletal response need be estimated. Effective stress mechanics also allows the modeler to have greater confidence in the accuracy of the results, since the complicated interactions of the material phases are treated in a more consistent manner than in a total stress approach. For example, with a model fit to relatively low-pressure drained laboratory test data, saturated-undrained material responses may be predicted at stress levels much higher than the available laboratory data. A total stress model would be limited to the maximum stress level obtainable in the laboratory. As another example, the hysteresis observed during the undrained hydrostatic loading of fully saturated materials and caused by occluded porosity may be simulated by using a hysteretic grain compressibility model.

The use of a modified Biot theory has several advantages. This theory incorporates all of the advantages of effective stress mechanics, i.e., all of the material constituents may be explicitly treated. Due to the coupled nature of the theory, pore pressure is a calculated degree of freedom. Thus, any skeletal constitutive model may be used in the solution scheme. The constitutive model is not directly responsible for calculating pore fluid pressures; it is responsible for

determining the effective or skeletal stresses. The coupled solution scheme significantly increases the number of available material models in comparison to uncoupled effective-stress solution schemes. Constitutive models ranging from linear elastic and hyperbolic models to cap and microplane models can be implemented in a coupled solution scheme. Using Biot's theory, it is also possible to calculate the time dependent flow of pore fluids in porous media. This was a required feature in the analysis tool. Since several researchers have already developed finite element formulations of Biot's theory (see next section) a finite element formulation was adopted as the solution scheme in this research.

3.3 Background

In 1941, Biot published his three-dimensional theory of consolidation for static loading. In his theory, Biot coupled the solution of the equations of pore fluid diffusion with the equations of deformation for the porous solids. He was thus able to calculate time-dependent displacements, strains, pore fluid pressures, and effective stresses. Biot made the following assumptions in his formulation: (1) the material was isotropic, (2) the material was linear elastic, (3) small strains were applicable, (4) the pore water was incompressible, (5) the pore water could contain air bubbles, and (6) flow of the pore water obeyed Darcy's Law. In subsequent papers, Biot extended his theory to include anisotropic materials, viscoelastic materials, and dynamic processes (Biot 1955; 1962).

With the rapid development of digital computers and advances in numerical techniques such as the finite element method, many investigators expanded Biot's theory in attempts to model more realistic and more complex problems. Sandhu and Wilson (1969) were the first to use finite element techniques with Biot's original formulation to solve initial boundary value problems. They applied variational principles to the field equations of fluid flow in a fully saturated porous elastic continuum, and then used the finite element method to numerically solve the resulting coupled equations.

Ghaboussi and Wilson (1972, 1973) developed a variational formulation of Biot's dynamic field equations for saturated porous elastic solids. Their finite element formulation allowed for the compressibilities of both the fluid and solid phases. Their methods were applicable to dynamic soil-structure interaction and wave propagation problems in saturated geologic media.

Zienkiewicz and his colleagues have written extensively about their use of modified versions of Biot's formulation to solve consolidation, liquefaction, and wave propagation problems in fluid saturated porous materials (Simon *et al.* 1986a and 1986b; Zienkiewicz 1985a; Zienkiewicz *et al.* 1980; Zienkiewicz and Shiomi 1984). They have incorporated several different nonlinear constitutive models into their numerical codes. For example, Lewis *et al.* (1976), used a hyperbolic constitutive relationship to model the skeletal response of the solids. They incorporated fluid and solid compressibilities, creep, and void ratio dependent permeability into their code. Zienkiewicz and his colleagues have also demonstrated a capability to solve dynamic problems such as ground motions due to earthquakes. For example, Zienkiewicz *et al.* (1982), modified the Critical State model to include a Coulomb-type failure surface and incorporated a "cumulative densification" feature into the constitutive model that allowed pore fluid pressures to increase with increasing numbers of load-unload cycles. They then demonstrated the utility of their approach when they used their code to approximate the earthquake induced displacements and pore pressures within the Lower San Fernando Dam.

Other investigators have also expanded Biot's formulation with nonlinear constitutive models. Oka *et al.* (1986) developed an elasto-viscoplastic constitutive model for clay and used Biot's theory to study the two-dimensional consolidation response of sensitive and aged clay deposits. They demonstrated the capability of their code to simulate the consolidation response of clay deposits during the construction phase of embankments. Chang and Duncan (1983) used a modified Cam Clay constitutive model in their analyses of earth structures constructed of compacted, partially saturated clay soils. They also applied the concept of a "homogenized pore fluid" to Biot's formulation in order to model partially saturated clay soils. With this implementation, they were able to treat partially saturated soils as two-phase materials, i.e., solids

and compressible pore fluid, instead of using a more theoretically rigorous approach involving three-phase materials.

Lewis and Schrefler (1987) extended Biot's formulation to include the governing equations for single phase, multiphase, and saturated-unsaturated flow in a deforming porous solid. They discussed finite element procedures for both the space and time discretization aspects of consolidation problems. They also presented linear elastic and nonlinear constitutive relationships; the nonlinear models included the hyperbolic model and incremental elastic-plastic models such as the Critical State models.

3.4 Finite Element Formulation

3.4.1 Effective stresses and strains

For a nonlinear material not susceptible to creep strains, a general stress-strain relation can be written as

$$\begin{aligned} d\sigma_{ij}' &= D_{ijkl}\left(d\varepsilon_{kl} - d\varepsilon_{kl}^{g} \right) \\ &= D_{ijkl}\, d\varepsilon_{kl}' \end{aligned} \qquad 3.1$$

where σ_{ij}' is the effective stress tensor, D_{ijkl} is the fourth-order tangential stiffness tensor or constitutive matrix, ε_{kl} is the total strain tensor, ε_{kl}^{g} is a tensor of strains due to the compression of the grains by the pore fluid, and ε_{kl}' is the effective strain tensor. The concept of effective strains is important in understanding the effective stress environment of porous materials subjected to high pressure loadings under undrained boundary conditions. The incremental tensor $d\varepsilon_{kl}^{g}$ is the key component in determining effective strains and it is evaluated as

$$d\varepsilon_{kl}^{g} = - \frac{d\pi}{3K_g} \delta_{kl} \qquad 3.2$$

where K_g is the bulk modulus of the grains, π is the pore fluid pressure, δ_{kl} is the Kronecker delta defined by

$$\delta_{ij} = \begin{cases} = 1 & \text{if} \quad i = j \\ = 0 & \text{if} \quad i \neq j \end{cases}$$

and an engineering mechanics sign convention is used in which compression is negative.

The concept of effective strains and the purpose of the term $d\varepsilon_{kl}^{g}$ are illustrated in the following example. If a porous specimen surrounded by a pervious membrane was placed into a pressure vessel and a pressure of several hundred megapascals was applied, a volume decrease would be measured in the specimen due to the compression of the grains. However, since the increments of total strain $d\varepsilon_{kl}$ are equal to the increments of volume strain due to grain compressibility, i.e., $d\varepsilon_{kl} = d\varepsilon_{kl}^{g}$, the effective strains and therefore the effective stresses within the specimen are zero. The concept of effective strains dictates that under drained boundary conditions, the total and effective strains are equal, and therefore the total and effective stresses are equal. Under undrained boundary conditions, the total and effective strains are not equal, and the effective stresses are a function of the effective strains, not the total strains. With the term $d\varepsilon_{kl}^{g}$ included in the general stress-strain relation, effective stresses can simply be calculated as

$$d\sigma_{ij}' = d\sigma_{ij} + d\pi \delta_{ij} \qquad 3.3$$

In Equation 3.3, no factor need be applied to the pore pressure term to account for grain compressibility, which was a method proposed by Skempton (1960). After appropriate manipulation, the above equations will yield Skempton's equation

$$\Delta p' = \Delta p - \left(1 - \frac{K}{K_g} \right) \Delta \pi \qquad 3.4$$

where p is pressure, K and K_g are the bulk modulus of the skeleton and grain solids, respectively.

3.4.2 Finite element equations

The general equations developed from the spacial discretization of the equilibrium and continuity equations have been documented by a large number of investigators (Lewis and Schrefler 1987; Zienkiewicz 1985a). Lewis and Schrefler developed the following equations

$$[K]\dot{u} - [L]\dot{\pi} - \dot{R} = 0 \qquad 3.5$$

and

$$[H]\pi - [S]\dot{\pi} - [L]^T \dot{u} - Q = 0 \qquad 3.6$$

where [K] is the tangent stiffness matrix of the solid phase,

$$K = \int_\Omega B^T D_T B \, d\Omega \qquad 3.7$$

[L] is the coupling matrix between the solid and fluid phases,

$$L = \int_\Omega B^T \boldsymbol{m} \bar{N} \, d\Omega - \int_\Omega B^T D_T \frac{\boldsymbol{m}}{3K_g} \bar{N} \, d\Omega \qquad 3.8$$

[H] is the permeability matrix of the porous skeleton,

$$H = \int_\Omega (\nabla \bar{N})^T \frac{k}{\mu} \nabla \bar{N} \, d\Omega \qquad 3.9$$

[*S*] is the compressibility matrix,

$$S = \int_{\Omega} \bar{N}^T s \, \bar{N} \, d\Omega \qquad 3.10$$

in which the scalar *s* is evaluated as

$$s = \frac{1 - \varphi}{K_g} + \frac{\varphi}{K_f} - \frac{1}{(3K_g)^2} \boldsymbol{m}^T D_T \boldsymbol{m} \qquad 3.11$$

R is the external force vector,

$$R = \int_{\Omega} N^T d\boldsymbol{b} \, d\Omega + \int_{\Gamma} N^T d\hat{\boldsymbol{t}} \, d\Gamma \qquad 3.12$$

Q is the vector of boundary flows,

$$Q = \int_{\Gamma} \bar{N}^T q \, d\Gamma + \int_{\Omega} (\nabla \bar{N})^T \frac{k}{\mu} \nabla \rho g h \, d\Omega \qquad 3.13$$

and the superimposed dot indicates a time derivative. In the above equations, $\dot{u}$ is the vector of displacement increments, $\dot{\pi}$ is the vector of pore pressure increments, D_T is the elastic-plastic constitutive matrix, $\boldsymbol{m}$ is the matrix equivalent of the Kronecker delta, *B* is the strain-displacement matrix, *N* is the matrix of displacement shape functions, $\bar{N}$ is the matrix of pore pressure shape functions, $\boldsymbol{b}$ is a vector of body forces, $\hat{\boldsymbol{t}}$ is a vector of surface tractions, *k* is the absolute permeability matrix of the material, μ is the dynamic viscosity of the pore fluid, K_g and K_f are the bulk modulus of the grain solids and pore fluid, respectively, φ is the porosity of the material, *q* is the vector of applied fluid flux, and ρ, *g* and *h* are fluid density, gravity, and elevation head, respectively.

Modifications were made to Equations 3.8 and 3.11 following the arguments presented in Appendix A; these equations are rewritten below

$$L = \int_{\Omega} B^T \boldsymbol{m} \bar{N} \, d\Omega \tag{3.14}$$

and

$$s = \frac{1 - \varphi}{K_g} + \frac{\varphi}{K_f} \tag{3.15}$$

Although numerous papers pertaining to the FE equations governing pore fluid flow in a deforming porous solid are available, none outline the equations required to calculate the residual forces. In Appendix B, these equations are developed for a nonlinear incremental finite element program that employs a modified Newton-Raphson solution scheme. The initial and final equations are summarized below.

The time integration of Equations 3.5 and 3.6 is performed using the following approximation

$$\int_t^{t+\Delta t} \chi \, dt = \alpha \Delta t \, {}^{t+\Delta t}\chi + (1 - \alpha) \Delta t \, {}^{t}\chi \tag{3.16}$$

for $0 \le \alpha \le 1$. From Equation 3.16, the following are developed

$${}^{t+\alpha\Delta t}\dot{\chi} = \frac{{}^{t+\Delta t}\chi - {}^{t}\chi}{\Delta t} \tag{3.17}$$

and

$${}^{t+\alpha\Delta t}\chi = (1-\alpha) \, {}^{t}\chi + \alpha \, {}^{t+\Delta t}\chi \tag{3.18}$$

Table 3.1.
Time Integration Parameters

Value α	Difference Scheme	Stability
0	Forward or Euler	Conditionally
½	Crank-Nicolson	Unconditionally
⅔	Galerkin	Unconditionally
1	Backward	Conditionally

Table 3.1 gives the most common difference schemes adopted by the selection of a given value of α.

The final equations written in matrix form for increment $t+\Delta t$ are

$$\begin{bmatrix} K & -L \\ -L^T & -S+\alpha\Delta t H \end{bmatrix} \begin{Bmatrix} \delta u^{(i)} \\ \delta\pi^{(i)} \end{Bmatrix} = \begin{Bmatrix} R - F^{(i-1)} + C^{(i-1)} \\ P - \Delta t[H]\pi^{(0)} - G^{(i-1)} + M^{(i-1)} \end{Bmatrix} \tag{3.19}$$

where *i* represents the current iteration,

$${}^{t+\Delta t}F^{(i-1)} = \int_V B^T \, {}^{t+\Delta t}\sigma^{(i-1)} \, dV \ ,$$

$${}^{t+\Delta t}C^{(i-1)} = {}^{t+\Delta t}[L]^{(i-1)} \, {}^{t+\Delta t}\pi^{(i-1)} \ ,$$

$${}^{t+\Delta t}G^{(i-1)} = \left\{ - {}^{t+\Delta t}[S]^{(i-1)} + \alpha\Delta t \, {}^{t+\Delta t}[H]^{(i-1)} \right\} {}^{t+\Delta t}\Delta\pi^{(i-1)},$$

$${}^{t+\Delta t}M^{(i-1)} = {}^{t+\Delta t}[L]^{T(i-1)} \, {}^{t+\Delta t}\Delta u^{(i-1)} \ ,$$

$${}^{t+\Delta t}\Delta\pi^{(i-1)} = {}^{t+\Delta t}\pi^{(i-1)} - {}^{t+\Delta t}\pi^{(0)} \ ,$$

$${}^{t+\Delta t}\Delta u^{(i-1)} = {}^{t+\Delta t}u^{(i-1)} - {}^{t+\Delta t}u^{(0)} \ ,$$

$${}^{t+\Delta t}\Delta u^{(0)} = 0 \ \text{ and } \ {}^{t+\Delta t}\Delta\pi^{(0)} = 0 \ ,$$

$$\delta u^{(i)} = {}^{t+\Delta t}u^{(i)} - {}^{t+\Delta t}u^{(i-1)} \ \text{ and } \ \delta\pi^{(i)} = {}^{t+\Delta t}\pi^{(i)} - {}^{t+\Delta t}\pi^{(i-1)} \ .$$

This is the system of equations that must be solved to calculate displacements and pore fluid pressures in a deforming porous solid.

3.5 Constitutive Models

Four of the five constitutive models available in the FE code JAM were developed by Owen and Hinton (1980). These models were implemented by Owen and Hinton in the FE code PLAST, which was the original FE code on which JAM was built. Each of the four models were implemented as elastic-plastic models with linear strain hardening, and each has a different yield criteria. The four models include the Tresca and von Mises criteria, which are suitable for metal plasticity, and the Coulomb and Drucker-Prager criteria, which are more suitable for the simulation of soil, rock, and concrete.

The yield stresses in both the Tresca and von Mises criteria are independent of pressure, which makes these models unsuitable for simulating the pressure dependent material behavior exhibited by soil, rock and concrete. In contrast, yield stresses in the Coulomb and Drucker-Prager criteria are pressure dependent. For more information on these models, the reader should refer to Chapter 7 in Owen and Hinton (1980).

An elastic-plastic strain-hardening cap model was implemented in JAM to calculate the time-independent skeletal response of the porous solids. The cap model enables the FE code to model nonlinear irreversible stress-strain behavior and shear-induced volume changes. Chapter 4 contains extensive documentation on the cap model.

3.6 Introduction: Equations of State for Air, Water, and Solids

The materials of interest to this investigation include partially-saturated soil- and rock-like geomaterials and man-made concretes, grouts, and groutcretes. The equations developed from

the Biot theory require an expression for the bulk modulus of the pore fluid and the grain solids. To determine the bulk modulus of the pore fluid, the concept of a homogeneous pore fluid will be adopted to treat partially-saturated materials. This investigation will assume that the liquid within the pore space is water and the gas within the pore space is air. Thus, the pore fluid will be regarded as a compressible mixture of air and water. Based on the equations of state (EOS) for air and water, we will develop equations for the bulk modulus of this air-water mixture. The grain solids will be treated as either linear or nonlinear elastic materials or as nonlinear hysteretic materials; each method for calculating the bulk modulus of the grain solids will be described.

3.7 Equation of State for Water

Over the pressure range of interest to this investigation, i.e., 0 to 600 MPa, water has a finite compressibility and should be treated as a nonlinear elastic compressible material. The compressibility of water is depicted in Figure 3.1 as a plot of pressure versus volumetric strain. Figure 3.1 also presents compressibility data for carbonate, steel, quartz, and granite. The reader should note that at 600 MPa the volume strain of water is nominally 14 percent. The bulk modulus or compressibility of water was evaluated from the Walker-Sternberg EOS for water (Walker and Sternberg 1965), which is valid for pressure levels of up to 50 GPa. The EOS expresses the water pressure as an analytical function of the density and the internal energy of the water. For this investigation, the energy dependent terms in the EOS were not included due to the assumed quasi-static and isothermal nature of the intended calculations. Without the energy terms, the EOS is expressed as

$$P = \rho f_1 + \rho^3 f_2 + \rho^5 f_3 + \rho^7 f_4 - P_0 \qquad 3.20$$

where P is the pressure in the water, ρ is the density of the water, f_i are material constants and P_0 is the initial pressure. If we define volumetric strain as

$$\varepsilon_{kk} = 1 - \frac{\rho_0}{\rho} \qquad 3.21$$

then the bulk modulus of water may be expressed as

$$K_w = \frac{dP}{d\varepsilon_{kk}} = \frac{\rho^2}{\rho_0}\frac{dP}{d\rho} \qquad 3.22$$

Substituting Equation 3.20 into Equation 3.22, one obtains the final expression for the bulk modulus of water as a function of density

$$K_w = \frac{1}{\rho_0}\left(\rho^2 f_1 + 3\rho^4 f_2 + 5\rho^6 f_3 + 7\rho^8 f_4\right) \qquad 3.23$$

In the FE program, pressure is the known quantity, not density. Since the EOS expresses pressure and bulk modulus as a function of density, Newton's method was used to calculate the density for a given pressure, then the bulk modulus was calculated.

3.8 Air-Water Compressibility

3.8.1 Background

The concept of a homogeneous pore fluid (HPF) was first introduced by Chang and Duncan (1977). In using their concept, one assumes that a three-phase material containing air, water, and solids may be replaced with a two-phase material containing a compressible pore fluid and solids. A partially-saturated material is transformed into a fully-saturated material with an HPF. Effective stress is calculated in the same manner as for a fully-saturated material, and the modulus of the pore fluid is calculated based on the modulus or compressibility of an air-water mixture. The concept is applicable to materials with saturation levels greater than 85 percent. At these levels of saturation, the air should be in the form of occluded bubbles uniformly distributed

throughout the water, and the air and water pressures should be identical. At lower saturation levels, one cannot guarantee that the air and water pressures will be the same.

The compressibility of air-water mixtures has been studied by several investigators. Bishop and Eldin (1950) examined non-zero total-stress friction angles measured during undrained shear tests. They attributed the observed behavior to incomplete saturation of test specimens. Using Boyle's and Henry's Laws, they developed expressions for the compressibility of an air-water mixture without accounting for surface tension effects.

Schuurman (1966) reviewed the work of previous investigators and concluded that surface tension effects must be included in an air-water compressibility formulation. Schuurman claimed to be the first to attempt such a formulation. Schuurman assumed that at saturation levels greater than 85 percent, the air existed in the form of bubbles. However, to account for surface tension, the radius of the air bubbles was required, yet little if any experimental data was available to provide this necessary information. Schuurman's formulation also differed from that of Bishop in that he wrote his expressions in terms of the current volume of air as opposed to the original volume, and he assumed the water was incompressible.

Fredlund (1976) also developed an expression for the compressibility of an air-water mixture using a formulation in which the water had a finite compressibility. He accounted for surface tension in a manner that did not require a knowledge of air bubble sizes by using a parameter for air-water pressures similar to Skempton's B parameter, which could be evaluated experimentally. Fredlund also interpreted the mixture volume in the expression for compressibility as the volume of water plus free air as compared to water plus total air.

Chang and Duncan (1977) based their expressions for the compressibility of an air-water mixture on the equations of Schuurman. Like Schuurman, they included surface tension effects in their formulation and assumed the water was incompressible.

Alonso and Lloret (1982) reviewed the work of previous investigators, compared the compressibility curves of each, and formulated their own expressions for the compressibility of an air-water mixture. They assumed a finite compressibility for water and accounted for surface tension in the same manner as Fredlund.

In summary, there are significant differences in the equations developed by several investigators for air-water mixtures. For this reason, equations for the compressibility of an air-water mixture will be developed in this chapter. Prior to developing the equations, a brief description of the appropriate physical laws will be provided.

3.8.2 Boyle's and Henry's laws

Boyle's and Henry's Laws will be used in developing equations for the compressibility of an air-water mixture. These laws are defined and explained for purposes of completeness. Boyle's Law states that "at a constant temperature, the volume of a given quantity of any gas varies inversely as the pressure to which the gas is subjected" (CRC Handbook 1980).

Air dissolves in water according to Henry's Law, which states that "the weight of gas

Table 3.2.
Solubility of Air in Water

Temperature Degrees C	Henry's Constant
0	0.02918
4	0.02632
10	0.02284
15	0.02055
20	0.01868
25	0.01708
30	0.01564
from Fredlund (1976)	

dissolved in a fixed quantity of liquid, at constant temperature, is directly proportional to the pressure of the gas above the solution" (Fredlund 1976). Fredlund (1976) explains that the structure of water molecules produces a "porosity" within the water of approximately 2 percent by volume. This porosity can be filled by a gas such as air, i.e., air dissolves in water by filling this pore space (see Table 3.2). Fredlund (1976) provides a simple analogy to understand the compressibility of an air-water mixture. Consider a test vessel made of a cylinder and piston. At the base of the cylinder is a porous stone having a porosity of 2 percent; the porous stone simulates the behavior of the water. The piston is initially positioned some distance above the stone with air filling the space in between. An imaginary valve at the surface of the porous stone controls the movement of air into the stone. The air in the porous stone simulates the air dissolved in water. If the valve is closed and the piston moves down into the cylinder, the air above the stone compresses following Boyle's Law. If the valve is opened, some of the air will diffuse into the porous stone following Henry's Law. This process will continue until all of the air passes into the porous stone. When the piston contacts the porous stone, there is a discontinuity in the compressibility of the system; the compressibility jumps immediately to that of water. The level of saturation within an air-water mixture must be evaluated to determine the discontinuity point.

3.8.3 Derivation of equations

The following assumptions were made for this analysis. We will assume initial saturation levels are greater than 85 percent, which implies that all air bubbles are occluded. Surface tension effects will be neglected, which allows us to assert that the air bubbles within the water will be at the same pressure as the water. The air is soluble in water and observes Henry's Law, and the rate of increase in pore water pressure from any simulation is slower than the rate of diffusion of air in water. Finally, prior to full saturation, the compressibility or bulk modulus of water is a constant. The equations for an air-water system with a rigid porous skeleton and then one with a compressible porous skeleton are developed in detail in Appendix C.

The final expression for the level of saturation in a deforming porous skeleton is

$$S = \frac{V_w}{V_a' + V_w} = \frac{n_o S_o (1 - C_w \delta P)}{n_o - \varepsilon_{kk}} \qquad 3.24$$

where V_w is the volume of water, V_a' is the volume of free air, which is equal to V_a the total volume of air minus V_d the volume of dissolved air, n is the porosity, ε_{kk} is the effective volumetric strain, C_w is the compressibility of water, P is the pore fluid pressure, and a subscripted "o" is used to indicate an initial value. The equation for the compressibility of an air-water mixture within a deforming porous skeleton is written as

$$C_m = \frac{n_o}{n_o - \varepsilon_{kk}} \left\{ \frac{P_{ao}}{P_a^2} (1 - S_o + S_o H) + S_o C_w \right\} \qquad 3.25$$

where P_a is the pore air pressure and H is Henry's constant.

In the process of a calculation, one must first evaluate Equation 3.24. If the level of saturation is less than one, Equation 3.25 is used to calculate the bulk modulus of the pore fluid. If the level of saturation is equal to one, the bulk modulus of the pore fluid is calculated from the EOS of water, i.e., Equation 3.23.

To illustrate the response of a partially-saturated material to an applied loading, an example calculation was conducted and the output graphically presented in Figure 3.2. The simulated material has a Young's modulus of 1800 MPa, a bulk modulus of 1000 MPa, a total porosity of 20 percent, a saturation level of 90 percent, and an air porosity of 2 percent. The material was loaded under undrained uniaxial strain boundary conditions. At volume strains less than approximately 2 percent, the generated pore pressures are negligible, and the loading bulk modulus is equal to the skeletal bulk modulus of 1000 MPa. At these strains levels, the material loads as if it were fully drained. At a volume strain of 2 percent, all of the air porosity is eliminated, and the pore fluid becomes fully saturated and begins to carry a major portion of the

applied stress. At these strain levels and above, the material loads as a fully-saturated material. In addition, the pressure-volume response is nonlinear due to the nonlinear nature of the water.

3.9 Equation of State for Solids

Three methods for calculating the bulk modulus of the grain solids were implemented in the FE program. The first method assumes the grain solids are linear elastic materials. The second method uses an analytical EOS and treats the solids as a nonlinear elastic material. The third method uses a simple model to simulate the nonlinear hysteretic material behavior of the grains.

The first method is self explanatory; the program simply uses a constant bulk modulus value for the entire calculation. In the second method, an analytic relationship between pressure and compression is developed for each material. Compression is defined as

$$\mu = \frac{\varepsilon_v}{1 - \varepsilon_v} \tag{3.26}$$

where ε_v is the Cauchy or engineering volume strain. Using solid carbonate as an example material, the pressure-compression relationship is linear below 1.2 GPa and may be written as

$$P_g = 0.7\,\mu \tag{3.27}$$

where P_g is the grain pressure. The bulk modulus for carbonate may then be written as

$$K_g = (1 - \mu)^2 \frac{dP}{d\mu} = 0.7\,(1 - \mu)^2 \tag{3.28}$$

A plot of pressure versus volumetric strain for carbonate is plotted in Figure 3.3 Other materials may be simulated in an analogous manner.

The third model, which simulates nonlinear hysteretic material behavior, uses tabulated curves that describe the loading and unloading pressure-volume response of the grains. This model is based on the work of Meier (1986), who used a similar model for one-dimensional, plane-wave ground shock calculations.

During virgin loading, the volume strain is computed from the current value of pressure through linear interpolation of the tabulated loading curve. A similar process is employed when unloading occurs from pressure levels at or above the lockup point using the tabulated unloading curve. When unloading takes place from pressure levels below the lockup point, a scaling process must be applied to the tabulated unloading curve. In this scaling process, let P_m and ε_m represent the peak pressure and peak volume strain, respectively, from which unloading commences (see Figure 3.4). The pressure and volume strain scaling factors are calculated as

$$f_p = \frac{P_l - P_t}{P_m - P_t} \tag{3.29}$$

and

$$f_\varepsilon = (1 - a) f_p + a \tag{3.30}$$

where P_l is the pressure at lock up, P_t is the tension cutoff pressure, and a is an empirically determined calibration constant with values ranging between zero and unity. Knowing the unloading pressure (P_i), the recovered pressure (ΔP), which is the difference between the pressure at lock up and the value of pressure on the tabulated unloading curve, is calculated in the following manner

$$\Delta P = (P_m - P_i) f_p \tag{3.31}$$

The recovered strain ($\Delta\varepsilon$) is computed through linear interpolation of the tabulated unloading curve. The unloading volume strain (ε_i) is calculated by subtracting the scaled value of recovered strain from the peak strain

$$\varepsilon_i = \varepsilon_m - \frac{\Delta\varepsilon}{f_\varepsilon} \qquad 3.32$$

The bulk modulus on this unloading curve is calculated as

$$K_i = K_u \left(f_\varepsilon / f_p \right) = K_u \left(1 - a + \frac{a}{f_p} \right) \qquad 3.33$$

where $K_u = \Delta P / \Delta\varepsilon$. Reloading occurs along a line passing between the last unloading pressure-volume strain point and the point P_m, ε_m.

3.10 Element Implemented into JAM

A new element was implemented in JAM to calculate both the displacement and pore fluid pressures. JAM uses an eight-node isoparametric element with 16 displacement and four pore fluid degrees of freedom. Similar elements were used by Lewis and Schrefler (1987), Simon *et al.* (1986a; 1986b), Zienkiewicz (1985a), Zienkiewicz *et al.* (1980), and Zienkiewicz and Shiomi (1984). Four Gauss integration points are used in each element.

3.11 Summary

In this chapter, the work of Biot and other investigators was briefly described, followed by a discussion of the modified Biot equations implemented by Lewis and Schrefler and modifications that were made to those equations. In Appendix B, equations were derived for the

residual forces. The five constitutive models available in JAM and the element implemented into JAM were briefly described. The algorithms required to numerically simulate the behavior of the three primary constituents of geomaterials, air, water, and solids, were documented in this chapter. When these algorithms are combined with an appropriate skeletal model into the FE formulation of Biot's theory, the multikilobar response of any geomaterial may be calculated.

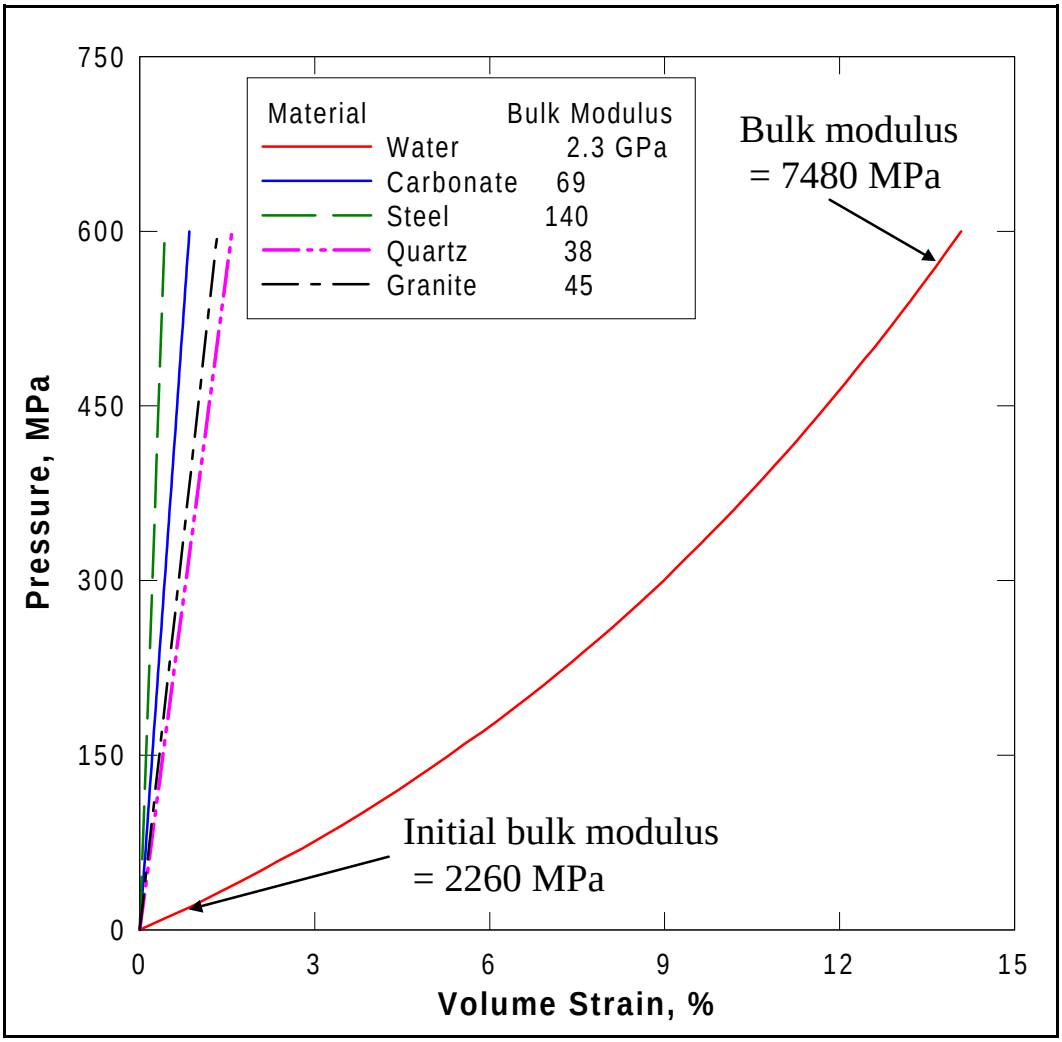

Figure 3.1. Pressure versus volumetric strain response of water

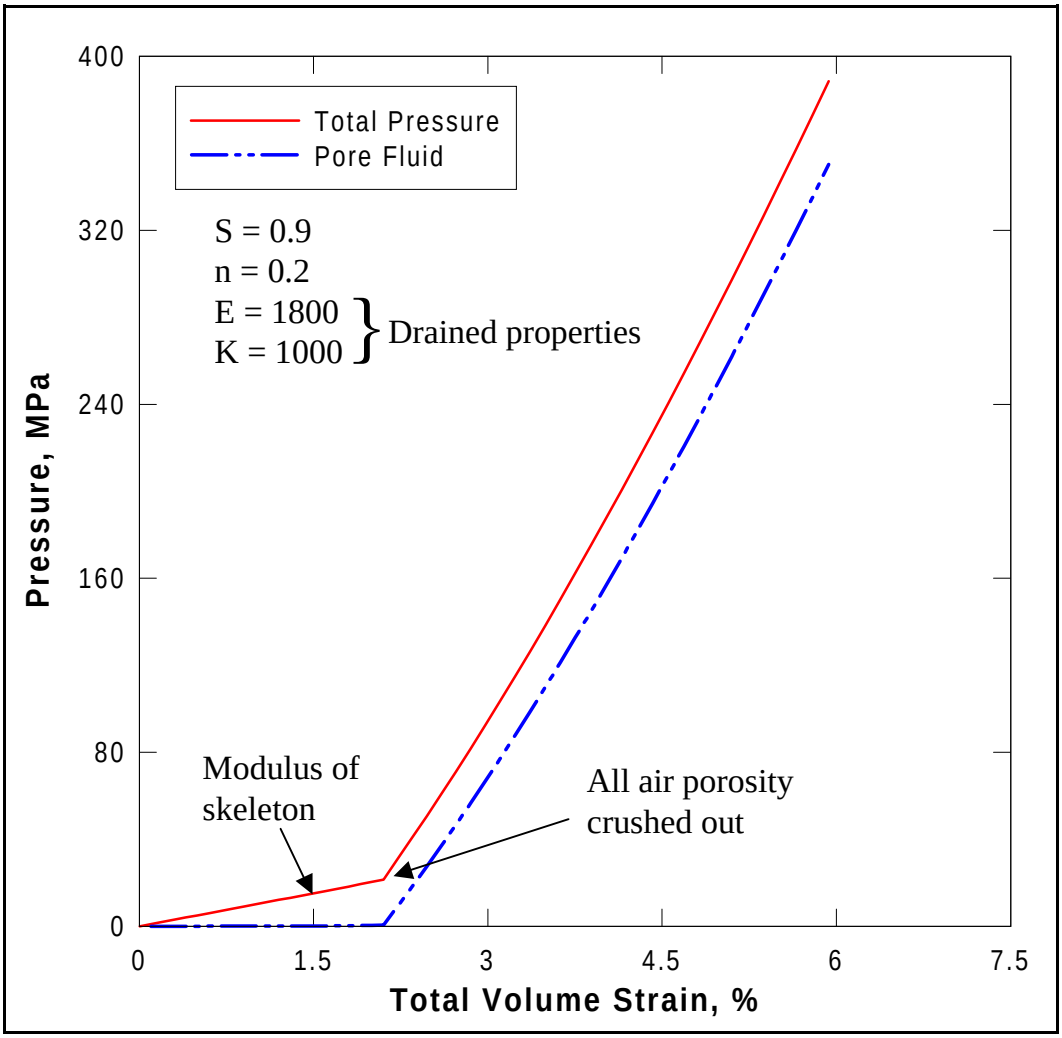

Figure 3.2. Pressure-volume response of partially-saturated material

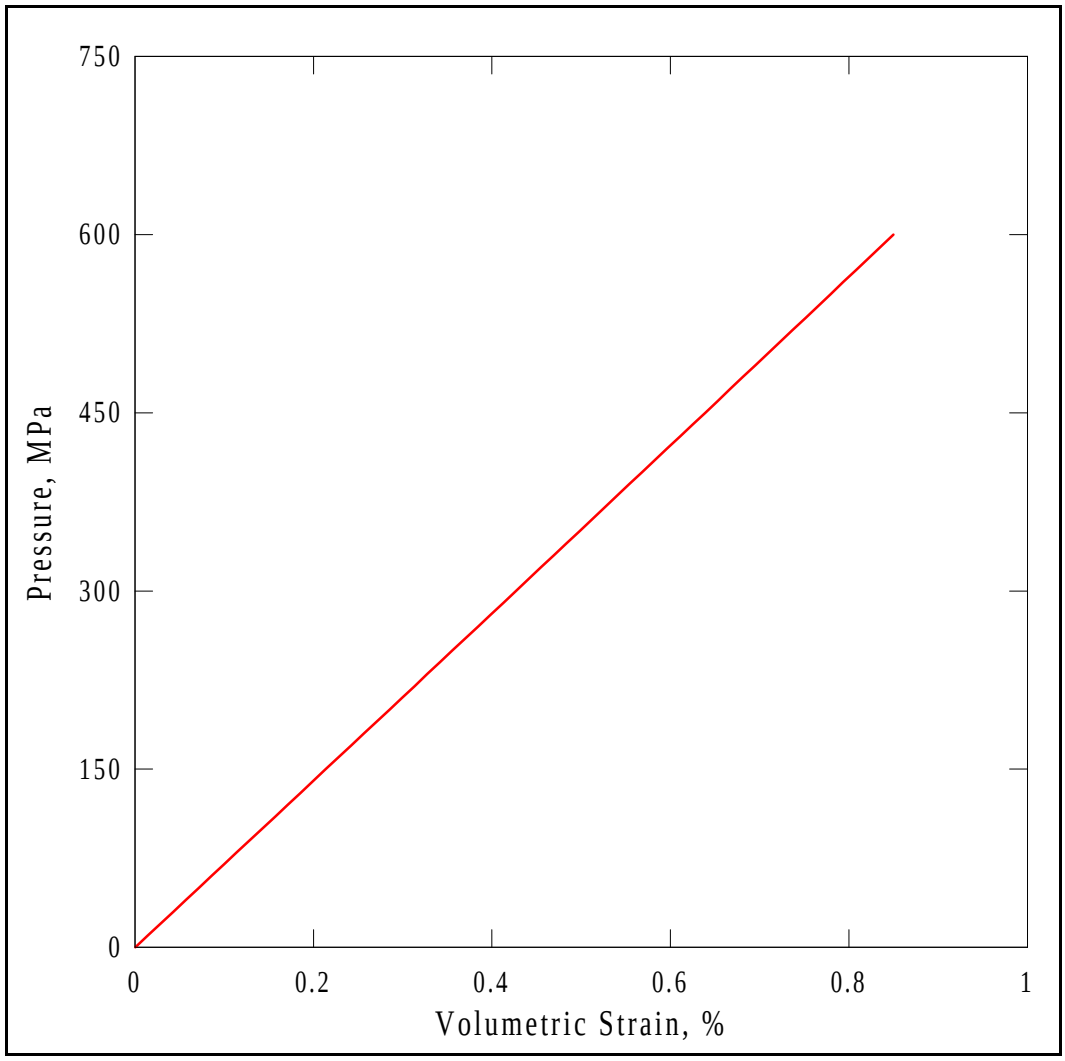

Figure 3.3. Pressure versus volumetric strain response of carbonate

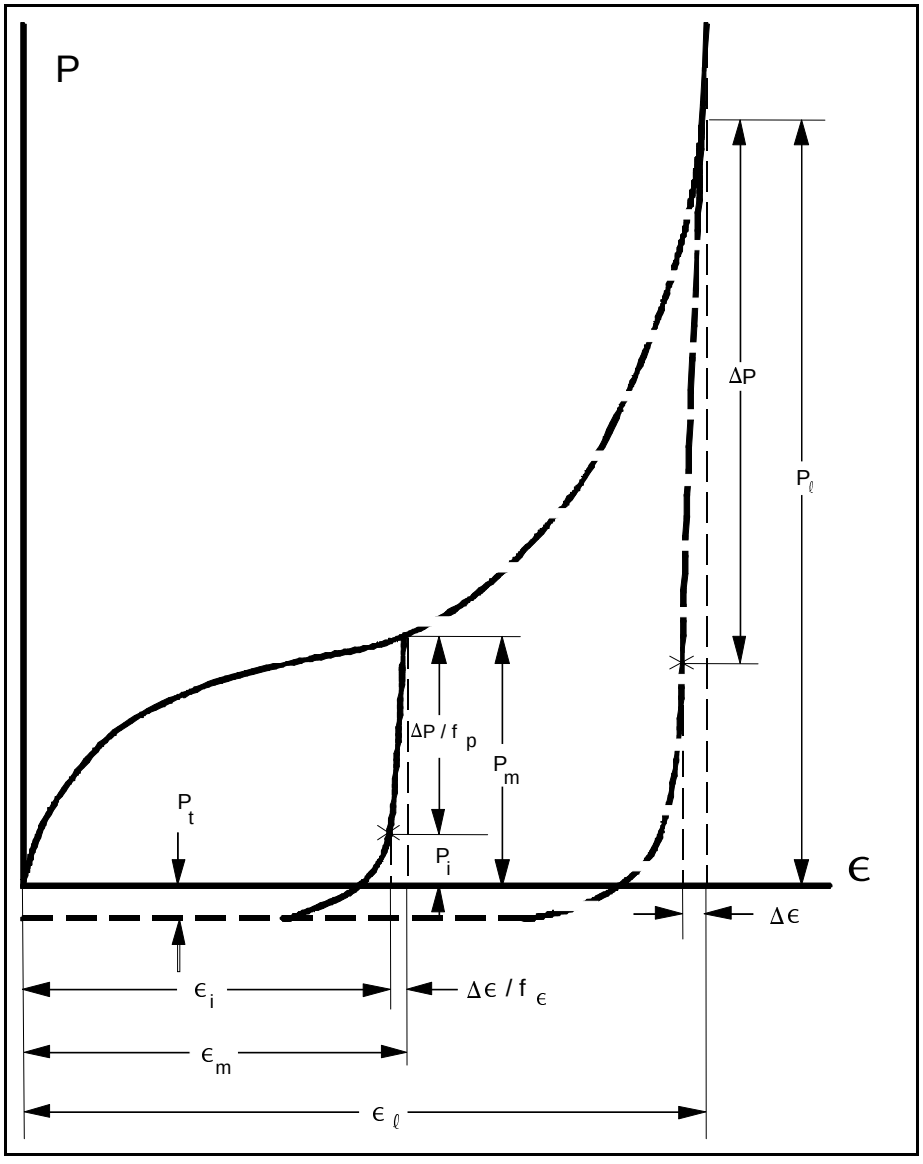

Figure 3.4. Nonlinear-hysteretic model